ELSEVIER

Biosensors & Bioelectronics 14 (1999) 377–386

BIOSENSORS & BIOELECTRONICS

Integrated optical surface plasmon resonance immunoprobe for simazine detection

R.D. Harris [a,*], B.J. Luff [a], J.S. Wilkinson [a], J. Piehler [b], A. Brecht [b], G. Gauglitz [b], R.A. Abuknesha [c]

[a] *Optoelectronics Research Centre, University of Southampton, Southampton SO17 1BJ, UK*
[b] *Institut für Physikalische und Theoretische Chemie, Eberhard-Karls-Universität, Auf der Morgenstelle 8, D-72076 Tübingen, Germany*
[c] *Division of Life Sciences, King's College, University of London, Kensington London W8 7AH, UK*

Received 2 September 1998; accepted 20 January 1999

Abstract

This paper presents the detailed design and characterisation of a regenerable integrated optical surface plasmon resonance immunoprobe as a detector for the triazine herbicide simazine. A sensor design theoretically optimised for use in the aqueous environment is presented and its fabrication described. Experimental results on the sensitivity to changes in bulk refractive index of the analyte and on non-specific binding of ovalbumin are presented. Binding inhibition immunoassays were conducted for simazine and the lower limit of detection determined to be 0.16 μg/l using anti-simazine IgG antibodies and 0.11 μg/l using anti-simazine Fab fragments. A sample test cycle of 20 min was established.

Keywords: Surface plasmon resonance; Integrated optics; Immunoprobe; Environmental monitoring

1. Introduction

Pesticides are in widespread use in agriculture to increase crop yields, and triazine based compounds are commonly employed as herbicides throughout the world. Concerns about their toxicity and persistence in the environment has led to a ban on one of the more heavily used triazines, atrazine, in more than one country, for instance, Germany and Sweden (Watterson, 1991; Bester & Hühnerfuss, 1993). The persistence and mobility of the triazine herbicides is amply demonstrated by the existence of measurable quantities of atrazine and simazine in the Elbe Estuary in the North Sea (Bester and Hühnerfuss, 1993).

The European Community has set limits on the concentrations of pesticides that may exist in ground and surface water (European Community, 1980). These concentrations are 0.1 μg/l for a single pesticide and 0.5 μg/l for the combined total of pesticides. Laboratory based techniques, such as high pressure liquid chromatography (HPLC) and gas chromatography with mass spectroscopy (GC-MS), exist that readily detect pesticide concentrations at the 0.1 μg/l level and below. These techniques are usually expensive and time-consuming to use due to the need for sample treatment prior to analysis. There is a need for instrumentation that will allow the rapid in-situ analysis of water samples for pesticide contamination at low cost. Immunoassay techniques offer one route towards this goal. Laboratory based enzyme-linked immunosorbent assay (ELISA) test kits for the detection of triazine herbicides are commercially available and have been validated with natural water samples (Mouvet et al., 1995). When coupled with an optical transducer, a label-free, lightweight, rugged and simple biosensor can be developed. Several types of optical transduction mechanisms have been utilised in biosensors, although the refractometer is one of the more common. Optical biosensors based on surface plasmon resonance (SPR) (Minunni and Mascini, 1993), grating couplers (Lukosz, 1991a; Lukosz et al., 1991b; Bier and Schmid, 1994), Mach-Zehnder interferometers (Heideman et al., 1993; Ingenhoff et al., 1993; Drapp et al., 1997), differ-

* Corresponding author. Tel.: +44-1703-593088; fax: +44-1703-593149.
E-mail address: rdh@orc.soton.ac.uk (R.D. Harris)

0956-5663/99/$ - see front matter
PII: S0956-5663(99)00014-7

ence interferometers (Fattinger et al., 1993; Schlatter et al., 1993), directional couplers (Luff et al., 1996a,b), reflectance interferometric spectroscopy (RIFS) (Brecht et al., 1995; Mouvet et al., 1996) and the resonant mirror (Goddard et al., 1994) have all been reported in the literature. At the present time several laboratory based biosensors utilising optical transduction techniques are available commercially. These include the Biacore 'bulk', prism based, SPR system (Biacore AB, Uppsala, Sweden), the IAsys resonant mirror sensor (Affinity Sensors Ltd., Cambridge, UK) and a grating coupler sensor (ASI, Zurich).

Validation of a SPR biosensor in an integrated optical format (IOSPR) has been reported (Harris et al., 1995a, 1996; Mouvet et al., 1997). The use of an integrated optical form of biosensor allows for ready miniaturisation, multiplexing and ruggedisation. Employment of a metal-film in a IOSPR sensor also offers the possibility of electrochemical control of a sensing reaction, for instance (Lavers et al. 1995). In this paper we present the detailed design, fabrication and characterisation of this promising new IOSPR biosensor.

2. Principles of operation

2.1. Transducer design and operation

A schematic representation of a practical IOSPR biosensor is shown in Fig. 1. The basis of the sensor is a single mode waveguide produced, for example, by thermal ion-exchange in a glass substrate. A small region of the waveguide is coated with a thin metal film; this metal-coated part of the sensor may support a surface plasmon and forms the interaction region with the material under test. The structure incorporates a 3 dB passive splitter for referencing purposes and is suitable for fibre pig-tailing. A single transverse magnetic (TM) mode is excited in the input waveguide. After passing through the 3 dB splitter this mode then couples across the step discontinuity between the metal-coated and uncoated waveguide regions exciting the normal modes of the metal-coated region. After propagating through the metal-coated region of the sensor these modes excite the single mode in the uncoated output waveguide.

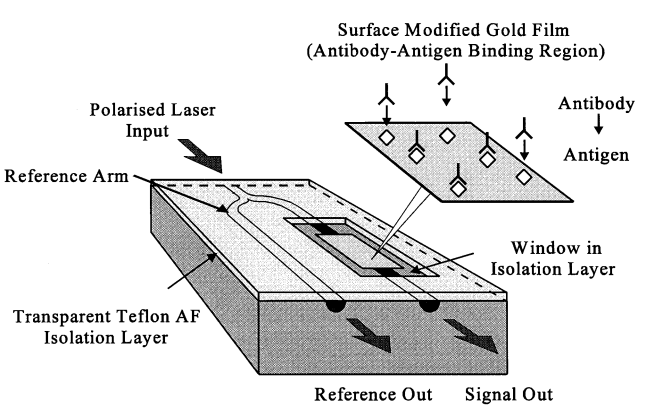

Fig. 1. Schematic diagram of the integrated optical SPR immunoprobe showing the binding of antibodies to the surface modified gold film.

Material such as a biomolecular layer adsorbed to the surface of the metal film will change the index of the superstrate within the evanescent fields of the normal modes propagating through the metal-coated structure. In turn, this will cause a change in the effective index of these modes leading to a change in the amount of power absorbed in the metal film or scattered at the end of the gold-coated region, manifested as a change in the transmission of the sensor. The basic sensing mechanism can then be summarised by stating that a change in the superstrate index close to the metal film of the sensor is detected as a change in output power of the sensor. Variations in input power, caused by changes in input coupling or light source power fluctuations, appear as noise on the measurement signal. The signal from the reference arm also contains these fluctuations and is used to ratio the measurement signal to reference them out. Only noise sources that are common to both arms of the sensor are removed by this referencing scheme.

A waveguide model to generate an optimal design of the IOSPR sensor was developed by Harris and Wilkinson (1995b). The model uses a planar waveguide approximation, treating the structure as a series of layers each with an homogeneous refractive index. The ion-exchanged waveguide is modelled as a single homogeneous slab. This is not the most accurate approach available but is certainly one of the most straightforward and, as well as providing physical insights into sensor operation, it leads to theoretical sensor designs that may be fine-tuned by experimental measurements (Harris, 1996b).

The model breaks the schematic sensor layout of Fig. 1 into two parts. First, a multilayer metal-coated part, which forms the active region of the sensor. Second, identical monomode input/output waveguides which couple light into and out of the multilayer region of the structure. In the multilayer structure the number of normal modes present are rigorously counted using the argument principle method (Delves and Lyeness, 1967) coupled with a transfer matrix approach to generate the system eigenvalue equation (Anemogiannis and Glytsis, 1992) and the complex modal effective indices are determined using Müller's method (Conte and de Boor, 1972). The input/output waveguide is then analysed to determine the effective index and field distribution of the mode supported by this waveguide and the excitation of the normal modes in the metal-coated region is calculated using the appropriate overlap integrals

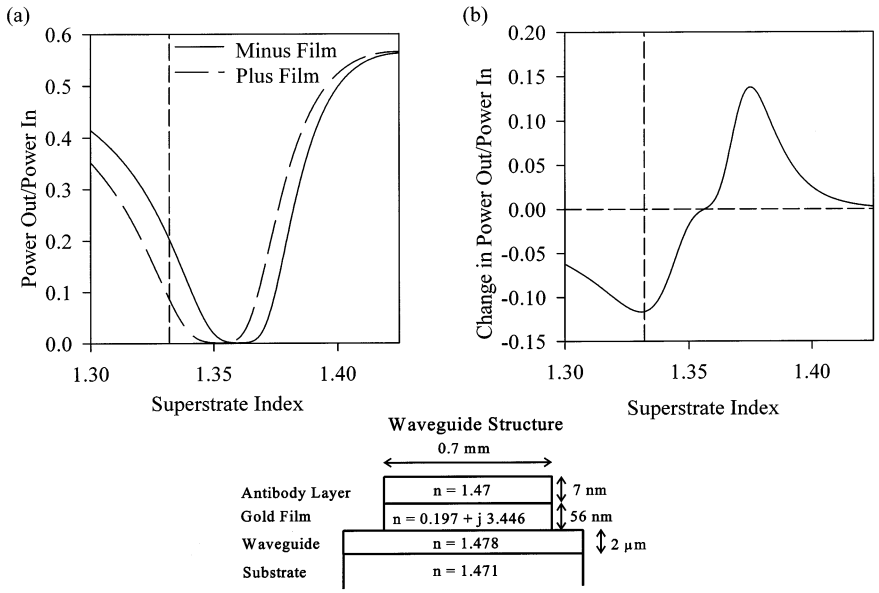

Fig. 2. Theoretical operating curves for a Pyrex IOSPR sensor at 633 nm incorporating a diagram of the waveguide structure modelled. The refractive index of water is shown as a dashed vertical line on each graph.

(Syms and Cozens, 1992). The normal modes are then allowed to propagate through the metal-coated region, where they undergo absorption and phase-shifts, before being recombined in the monomode output waveguide to determine the output power of the sensor.

The model was used to study the change in output power of the IOSPR sensor when a thin dielectric film is adsorbed to the surface of the metal film coating the waveguide. The parameters of the thin adsorbed film were chosen to represent a monolayer of IgG antibodies, representing the physical adsorption of antibodies to the surface of the sensor during an immunoassay. While this does not describe the mode of operation employed in the immunosensing experiments described below, it is expected to result in optimised designs for any sensing scheme which uses very thin surface films. Optimised sensor designs were identified using the model, based on the assumption that photodetector shot noise is the limiting factor in the sensitivity of the sensor. In reality, the practical stability of the sensor system, in terms of mechanical, thermal and wavelength drifts, is most likely to be the limiting factor in the sensitivity of the sensor. However, the photodiode shot noise is a rigorously defined quantity that may be applied as a sensitivity parameter in the sensor design process. This approach represents the attainable sensitivity if stability can be dramatically improved.

Fig. 2a plots the transmission of an IOSPR sensor optimised for the aqueous environment as a function of superstrate index before and after adsorbing such a thin dielectric film. The sensor structure and the parameters used in the waveguide model, are displayed in Fig. 2a, whilst the refractive index of water is indicated on the plot by a broken vertical line. On adsorption of the thin dielectric layer to the metal film the output power of the sensor falls by 58% at the refractive index of water. Fig. 2b plots the change in normalised output power of the sensor as a function of superstrate index, when the thin dielectric film is adsorbed to the surface of the metal film. The plot shows a high sensitivity close to the index of water but shows a region of higher sensitivity at a superstrate index of 1.375. It is possible to adjust the sensor design so that this second peak occurs near the index of water, by the inclusion of a dielectric buffer layer between the metal film and the waveguide (Harris and Wilkinson, 1995b). The increased complexity in fabrication of the sensor design that would result was deemed to outweigh the gain in sensitivity that could be achieved and has not been pursued.

2.2. Immunoassay format

The IOSPR biosensor described here has been configured to employ a binding inhibition assay, carried out in a two-step protocol, to measure the concentration of simazine in a water sample. The transducer surface was covalently modified to ensure optimum properties for long-term operation. A dextran layer was attached to the thiol-activated surface to reduce non-specific binding, providing a 3-dimensional matrix for immobilisation of the ligand. A triazine derivative with high affinity to the anti-simazine antibodies was attached to this matrix in high concentration. These conditions ensured high binding rates and diffusion-controlled binding at low antibody concentrations (Piehler et al., 1996) providing constant binding rates

even after partial degradation of the immobilised ligand (Brecht et al., 1995). Antibodies were mixed with standard simazine samples and the free antibody concentration was detected by exposing the samples to the modified surface in a flow-through format. Under these conditions the binding rate directly corresponds to the concentration of the free antibody and is therefore a measure of the simazine concentration in the sample. This constant rate of binding of antibodies to the sensor surface results in a constant rate of change of output power of the sensor and this rate forms the principal output parameter measured in the following experiments.

3. Experimental

3.1. Materials and devices

The preparation of triazine derivatives and of antibody and antibody Fab fragments and the affinity purification of IgG and Fab fragments have been described by Mouvet et al. (1995, 1996).

The transducer used in these experiments was realised as follows. Optical channel waveguides were fabricated by potassium ion-exchange in Pyrex glass substrates ($n = 1.471$) at a temperature of 385°C for 9 h. A 53 ± 3 nm gold film (Birmingham Metal, 99.99%) was deposited on the waveguides by thermal evaporation and patterned using conventional photolithography. The adhesion of the gold film to the glass substrate was improved by treating the glass substrate, prior to gold deposition, with (3-mercaptopropyl)trimethoxysilane in a similar manner to Goss et al. (1991). A 0.7 μm thick Teflon AF 1600 film (Du Pont, $n = 1.31$) was then deposited by thermal evaporation and patterned using lift-off photolithography (Luff et al., 1995), to create a window exposing the gold sensing surface. The gold surface was activated by treatment with a 0.1% mercaptopropionic acid in ethanol resulting in carboxy-functionalised surface. Amino dextran was attached to this surface using ethyl(dimethylaminopropyl)carbodiimide hydrochloride according to the process of Piehler et al. (1996). The triazine derivative 4-chloro-6-(isopropylamino)-1,3,5-triazine-2(6′-amino)caproic acid was coupled to the remaining amino groups using diisopropylcarbodiimide. At this point the activated immunoprobe was stable at room temperature for at least 1 month.

3.2. Experimental apparatus

Fig. 3 shows the experimental arrangement used for the characterisation of the SPR sensor as an immunoprobe. Light from a 10 mW, 632.8 nm, He–Ne laser was passed through a halfwave plate and Glan-Thompson polariser, for polarisation control, and end-fire coupled into a waveguide sensor which was overlaid with a 2.0 mm long gold film. Mechanical chopping of the laser beam allowed the use of lock-in amplifiers in the detector chain. The twin outputs from the device, from signal and reference arms, were focused onto a pair of silicon photodiodes, labelled PD1 and PD2 in Fig. 3 and the outputs were amplified before being acquired by the PC. The intensity output ratio of the device was then determined by dividing the measured output from the signal arm by that from the reference arm.

A wall-jet flow cell was clamped onto the waveguide under test on the substrate chip. The active cavity of the cell had a diameter of 12.5 mm and a depth of 75 μm, leading to a volume of 9.2 μl. The depth of the flow cell was maintained at 75 μm using a Mylar spacer onto which the flow cell was clamped. High density Teflon tubing connected the flow cell to a flow injection analyser (FIA) (Ismatec, Zurich). The PC used for data acquisition was also used to control the start of the FIA test-cycle. A background stream of phosphate buffered saline (PBS) having a pH of 7.4 was passed through the flow cell and over the gold film of the sensor under test to provide a stable operating environment for the sensor and biochemicals. The system was placed under a 0.5 bar excess pressure of argon gas to help eliminate air bubbles.

3.3. Sensor test procedures

3.3.1. Baseline drift and sensitivity to bulk index changes

The baseline drift of the output intensity ratio of the sensor was calculated from two sets of data recorded over 1 h with PBS flowing continuously over the sensor surface. Sensor sensitivity to bulk refractive index changes was determined by pumping a sucrose solution

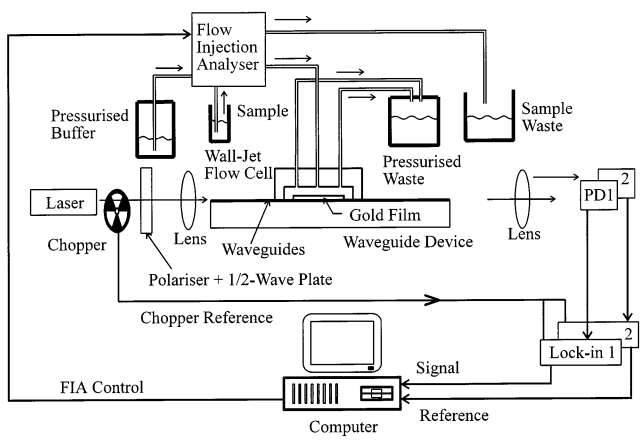

Fig. 3. Experimental set-up of the computer controlled FIA IOSPR immunoprobe system.

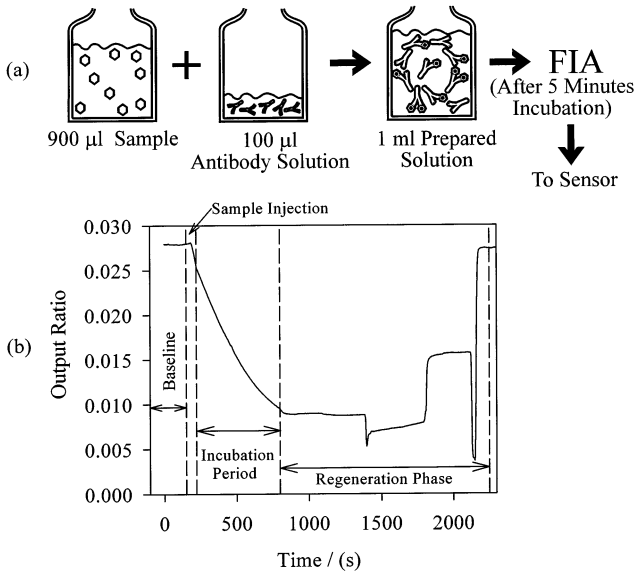

Fig. 4. IOSPR immunoprobe test-cycle: (a) Sample preparation; and (b) Sensor output ratio during the test-cycle.

with an index of 1.343 over the sensor surface and recording the change in output intensity ratio with respect to that for PBS. An Abbe refractometer operating at a wavelength of 589.3 nm was used to measure the refractive index of the sucrose solution.

3.3.2. Sensor response to specific and non-specific binding

The response of the immunoprobe to adsorption of a full antibody monolayer was measured by incubating a solution of 50 µg/ml anti-simazine IgG antibody at the sensor surface for 10 min. A suitable antibody concentration for subsequent simazine measurements was determined experimentally by reducing the concentration until linear binding of antibodies to the sensor surface was achieved; antibody concentrations of 5.0, 2.0, 1.0 and 0.35 µg/ml were applied. Non-specific binding effects of proteins were tested by a 10 min incubation of a solution of 1 mg/ml of ovalbumin in PBS at the sensor surface.

3.3.3. Immunoprobe response to simazine concentration

Calibration of the sensor as a simazine detector was carried out by performing repeated test-cycles using samples with a simazine concentration in the range 0.1–100 µg/l The following test protocol was established for use with anti-simazine IgG antibodies. 900 µl of PBS containing a known concentration of simazine was added to 100 µl anti-simazine IgG antibody solution to create a final sample volume of 1 ml, as shown in Fig. 4a. The sample was then incubated for 5 min to allow binding between the anti-simazine IgG antibodies and the simazine present in the sample to reach near equilibrium conditions. Following this incubation period the sample was loaded into the FIA system and injected into the flow cell on top of the sensor. During sample loading a measurement of the sensor output intensity ratio was recorded with PBS flowing over the sensor surface and this was recorded as the sensor baseline. Once the sample reached the flow cell it was incubated there for 10 min, at a flow rate of 10–20 µl/min to maintain a constant antibody concentration in the flow cell, before being washed out with PBS. After rinsing, the sensor surface was regenerated chemically by pumping various combinations of pepsin (2 g/l in PBS at pH 1.9) and a solution of 50% acetonitrile and 1% propionic acid in water over the sensor surface. An example test-cycle, showing the variation of the output intensity ratio of the sensor as a function of time using a 2 µg/ml anti-simazine IgG antibody solution as the sample is shown in Fig. 4b. The various stages of the test-cycle are labelled on the figure. It can be seen that the use of this high antibody concentration has led to a non-linear binding rate of antibodies to the sensor surface and so would not be used in an immunoassay. An antibody concentration of 0.35 µg/ml (2.3 nM) was used for determination of the calibration curves and a blank measurement, using a sample containing no simazine, was taken to complete each data set. Three complete calibration curves were obtained on three successive days using simazine concentrations of 0.0, 0.1, 0.32, 1.0, 3.2, 10.0 and 100.0 µg/1 prepared in PBS.

The characterisation of the immunoprobe was completed by obtaining a duplicate set of calibration data using a using a concentration of 0.33 µg/ml of Fab fragments of anti-simazine IgG antibodies instead of 0.35 µg/ml whole antibodies. The experiments using anti-simazine IgG antibodies described above were based on samples prepared in PBS. However, natural water samples must be buffered before they can be analysed in this immunoassay format. In preparation for future validation of the immunoprobe as a detector for simazine in natural water samples, test samples were prepared using deionised water, rather than PBS. In this case, 800 µl of sample in deionised water was buffered by the addition of 200 µl of five times concentrated PBS at pH 7.4. Then 900 µl of this buffered sample was added to the 100 µl of 0.33 µg/ml of Fab fragments to create a 1 ml buffered test sample. This gives rise to a final Fab fragment concentration of 6.6 nM. Two calibration curves were generated using the same test format as for those using whole IgG antibodies except that the incubation period was reduced from 10 to 8 min to expedite cycle times. The final cycle time including sample injection, incubation, washout, regeneration and re-establishment of the baseline was 20 min.

4. Results

4.1. Baseline drift and sensitivity to bulk index changes

Applying the sucrose solution, which had an index of 0.008 above that of the PBS background stream, to the sensor surface resulted in a 74.5% decrease in the output intensity ratio from 27.0×10^{-3} to 6.9×10^{-3}. An estimate of the sensitivity of the IOSPR sensor to bulk refractive index changes in the superstrate material can be made by comparing this change to the minimum resolvable change in output intensity ratio. The coefficient of variation (CV) of the baseline was calculated to be 0.32% over the measurement period of 1 h. On the basis of this measurement a minimum resolvable change in output intensity ratio, taken as three times the CV of the baseline, would be 0.96% of the initial baseline mean. Taking the approximation of a linear scaling of output ratio with superstrate index leads to a worst case estimate of a sensitivity with respect to superstrate index of 1×10^{-4} in the aqueous environment. Such a detection limit is approximately equivalent to a change in the temperature of the superstrate material, PBS, of 1 K (Weast, 1971).

4.2. Sensor response to specific and non-specific binding

Fig. 5 shows the change in the output ratio of the sensor when a 50 μg/ml solution of anti-simazine antibodies is incubated at the sensor surface for 10 min. The output ratio has become stable by the end of the incubation period, showing that surface coverage with antibodies has reached saturation. The full surface saturation of the IOSPR sensor with antibodies has shifted the output intensity ratio of the sensor through the point of maximum attenuation of the SPR curve. The estimated equivalent change in the bulk superstrate index is greater than 0.01.

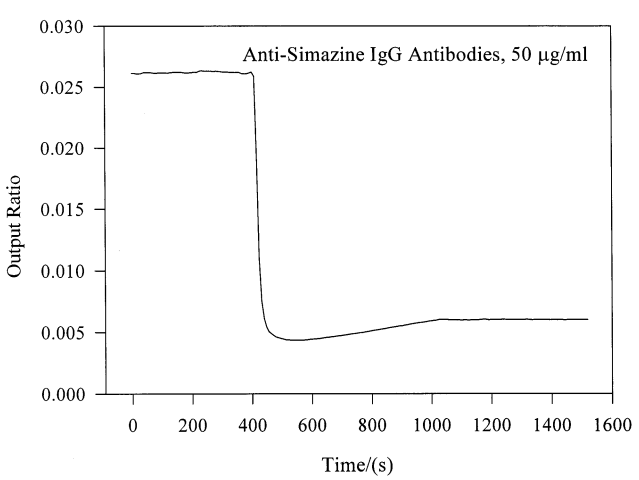

Fig. 5. Response to high anti-simazine IgG antibody loading of the sensor surface.

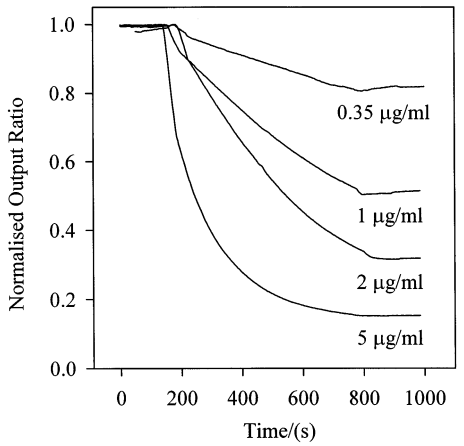

Fig. 6. System characterisation for reducing concentrations of anti-simazine IgG antibodies. A linear binding regime has been achieved by an antibody concentration of 0.35 μg/ml.

The variation in the sensor output ratio with time when solutions of varying antibody concentration were incubated at the sensor surface is shown in Fig. 6, each curve being labelled with the concentration of the corresponding antibody solution. The output ratio has been normalised to the maximum measured during each sample injection period. Reducing the concentration of the antibody solution caused a decrease in the change in sensor output ratio achieved during the incubation period. Further, as the antibody concentration decreases, the resultant binding curve more closely resembles a straight line. Eventually, when the concentration of incubated antibodies is sufficiently low, linear binding is achieved as antibody binding to the sensor surface becomes diffusion, rather than affinity, limited. The curve plotted for an antibody concentration of 0.35 μg/ml, or 2.3 nM based on a whole IgG antibody having a molecular weight of 150 000, shows near-linear behaviour. The root mean square value for the residuals of the linear regression of the binding curve, expressed as a percentage deviation from the fitted line, was calculated to be 0.26%.

Incubation of a 1 mg/ml sample of ovalbumin in PBS at the sensor surface led to a decrease in the output intensity ratio of 1.1% over the 10 min incubation period. This change in output intensity ratio is slightly greater than the minimum change resolvable by the sensor and shows that a very high concentration of ovalbumin solution leads to only a minor amount of non-specific binding of protein at the sensor surface.

4.3. Immunoprobe response to simazine concentration

A set of temporal responses of the immunoprobe to whole IgG antibody solutions preincubated with solutions of simazine of known concentration is shown in Fig. 7. The output ratio has been normalised to the

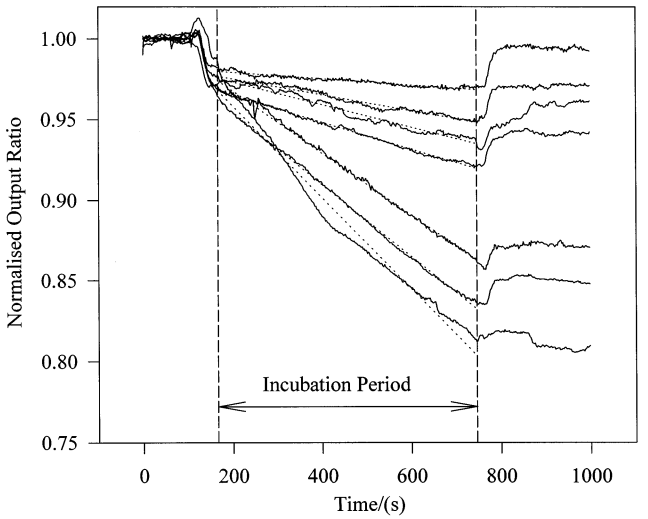

Fig. 7. Real-time immunoprobe response for several simazine concentrations over the range of 0–100 μg/l.

average of the baseline ratio (representing flowing PBS alone) over 100 s before sample injection at the beginning of each test-cycle. The slope of the steepest line represents the binding rate of the antibodies in the blank solution to the sensor surface. The curves in the middle of the plot represent simazine concentrations below 1 μg/l, whilst the smallest slope was recorded from the solution containing 100 μg/l of simazine. One complete simazine calibration curve was subsequently generated from this data set. The circled data points on Fig. 8 show the averaged triplicate calibration curve, using IgG antibodies, with a sigmoidal curve fitted to the averaged data set. The error bars on the data points represent one standard deviation of the mean of the

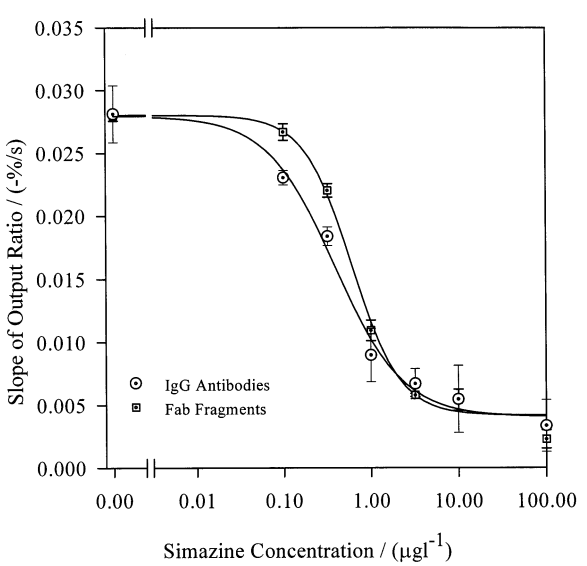

Fig. 8. IOSPR immunoprobe averaged triplicate anti-simazine IgG antibody calibration curve and averaged duplicate anti-simazine Fab fragment calibration curve.

averaged data points. The lower limit of detection of the sensor is found from the fitted curve, at that concentration where the binding slope has fallen to three standard deviations below the mean slope for the blank samples (Mouvet et al., 1996). Using this definition of sensitivity, the lower limit of detection for simazine was calculated to be 0.16 μg/l. The mid-point of the sigmoidal calibration curve was determined to be 0.39 μg/l, whilst the upper limit of the operating range of the sensor, represented by a binding slope value 90% below that of the blank sample, was 2.8 μg/l. Fig. 8 also shows the average of two calibration curves generated using the anti-simazine Fab fragments, the data points being represented by squares. The lower limit of detection for the sensor calculated from the fitted calibration curve is 0.11 μg/l, with a test mid-point of 0.61 μg/l.

Due to the nature of the laboratory environment in which these tests were performed, temperature changes were low and expected to occur over sufficient time not to influence the binding curve during an individual test-cycle. Over the period of a day, temperature fluctuations manifested themselves as drift in the baseline of the sensor, which would have resulted in a small change in sensitivity of the device.

5. Discussion

5.1. Sensitivity to bulk index changes

The IOSPR transducer demonstrated a detection limit for changes in bulk refractive index of 1×10^{-4} for measurements taken on the timescale of an hour. Theoretical consideration of noise equivalent power and sensitivity would predict a detection limit orders of magnitude lower than this. However, practical performance is limited by instabilities in the instrumentation, temperature and flow conditions, rendering comparisons of sensor performance difficult. A Mach-Zehnder interferometer sensor was reported by Heideman et al. (1993) to be capable of detecting a 4×10^{-6} change in superstrate index. The theoretical sensitivity of a difference interferometer to changes in superstrate index was calculated by Stamm and Lukosz (1993) to be 5×10^{-7}, but limitations in instrumental resolution led to a practical refractive index sensitivity of 10^{-5}. The IOSPR sensor reported here shows comparable performance in terms of bulk index detection limit, of 5×10^{-5}, estimated for a directional coupler sensor operating in the aqueous environment (Luff et al., 1996a). The principal sources of instability in the present measurements are believed to be fluctuations in temperature, which could be improved by temperature referencing or temperature control of the sensor surface and drift in the coupling of light into the device, which could be improved by fibre-coupling to the device. The

efficacy of referencing in the device may be limited by light launched into the substrate which is incident on the photodetectors and which fluctuates with input coupling. However, the estimated sensitivity of the IOSPR device is acceptable for the intended use of the sensor as a pesticide detector and could be readily improved by experimental tuning of the sensor structure and optimisation of the instrumentation. In contrast with conventional interferometers the sensitivity of this device cannot be increased simply by increasing the length of the interaction region. However, the short length of this sensor, 2 mm compared with the 10–20 mm used for the dielectric waveguide interferometers referred to above, provides potential advantages in terms of sample volume or integration of multiple sensors within a flow cell on a single optical chip.

5.2. Response to specific and non-specific binding

Full surface saturation of the sensor with anti-simazine antibodies resulted in a signal equivalent to that from a change in bulk index of more than 0.01, so the detection limit of the IOSPR sensor is below 1% antibody saturation. By comparison, a difference interferometer was reported as having a detection limit of 2 pg/mm^2 of IgG antibodies (Fattinger et al., 1993), corresponding to 0.04% of an antibody monolayer. In that case the signal was compared to drifts on a 10 min timescale, rather than the 1 h employed here. Further, the capture molecule was directly immobilised on the sensor surface, rather than on the dextran layer employed here to facilitate surface regeneration and the interferometer length was approximately 10 mm. Direct comparisons are therefore difficult to make but the detection limit appears to be roughly an order of magnitude better than the SPR sensor, as might be expected (Lukosz, 1991a). The degree of non-specific binding of proteins measured is considered to be negligible in terms of operation of this device for detection of pesticides in water.

5.3. Detection limit for simazine assays

The integrated SPR immunoprobe has shown lower limits of detection close to those required by EU legislation despite many aspects of the sensor and flow-cell design, sample handling and instrumentation requiring optimisation. The use of Fab fragments compared with whole antibodies resulted in a slight increase in test midpoint, due to a higher molar concentration of binding sites and a steepening of the calibration curve, due to the existence of a single binding site on the Fab fragment. The apparent difference in detection limit appears to be simply due to a lower standard deviation of the mean slope of the blank Fab fragment samples compared to that of the blank IgG samples. However, an advantage of using Fab fragments is that they do not contain the Fc portion of a whole IgG antibody, reducing non-specific adsorption to the sensor surface. The operation of the sensor as a simazine immunoprobe may be put into context by comparison with other optical pesticide sensors. One such device is the RIFS biosensor which employs changes in Fresnel reflection coefficients at the interface of a thin film to determine the presence of molecules at the sensor surface, (Brecht et al., 1995). A recent paper on the operation of a RIFS sensor showed a detection limit of 0.35 μg/l for atrazine detection, (Mouvet et al., 1996) which is comparable to that of the IOSPR sensor. Another useful comparison can be made between the IOSPR immunoprobe and the 'bulk' SPR approach as represented by the Pharmacia Biacore system which was used as an atrazine sensor, showing a limit of detection of 0.05 μg/l, a factor of 2–3 times better than the present device and a comparable mid-point of approximately 0.5 μg/l (Minunni and Mascini, 1993). The lower detection limit in a test with a similar mid-point is indicative either of more repeatable sample preparation or of the superior stability of the commercial SPR system. The IOSPR sensor may prove to have greater potential for miniaturisation and integration of sensor arrays than the bulk-optical system.

5.4. Outlook

The development of this integrated optical SPR immunoprobe into a system with a lower detection limit requires either an increase in the sensitivity of the transducer or improvements in the stability of the apparatus and repeatability of sample preparation. The sensitivity could be improved by the use of a buffer layer between the waveguide and gold film, or by fine-tuning of the present design. While significant improvements in transducer sensitivity are predicted, these devices are unlikely to compare with waveguide interferometers in this respect. However, it is expected that improved thermal and optomechanical stability, control of scattered light and reduction in fluctuations in the fluid handling will bring significant reduction in the lower detection limit. The present device has an advantage over the conventional interferometers, in that it uses a gold film for surface attachment, which may result in improved chemical stability and would allow electrochemical measurements. Furthermore, this device is substantially shorter than the interferometers and has an active area of approximately 0.01×2 mm, allowing the use of small sample volumes and the integration of multisensor arrays in small areas.

6. Conclusions

A chemically regenerable integrated optical SPR immunoprobe for the triazine herbicide simazine has been designed and fabricated and characterised using both anti-simazine IgG antibodies and their Fab fragments. Preliminary measurements showed that the transducer could detect a minimum change in the bulk superstrate index of 1×10^{-4}, at the refractive index of water, in the presence of the drifts observed on a 1 h timescale. The immunoprobe was calibrated with standard simazine solutions using anti-simazine IgG molecules and the calibration curve exhibited a mid-point of 0.4 μg/l and a lower limit of detection of 0.16 μg/l. The same device showed a mid-point of 0.61 μg/l and a lower limit of detection of 0.11 μg/1 when characterised using Fab fragments of the IgG antibodies. Regeneration of the immunoprobe allowed repeated assays at a cycle time of 20 min. These trials have demonstrated that the integrated optical SPR immunoprobe is suitable for the sensitive monitoring of immunobinding reactions in real time.

The estimated detection limit for the sensor is close to the EU limit of 0.1 μg/l for an individual pesticide in water. However, the EU has specified that the sum of all triazine herbicides and their metabolises may not exceed a concentration of 0.5 μg/1 in drinking water supplies. The immunoprobe reported here meets this specification and thus the sensor may potentially be employed as a screening tool for the combined triazine content of water samples. The short test duration and lack of sample pre-treatment is attractive compared to the time and sample requirements for other laboratory based tests such as HPLC. Further improvements in device design and system stability are expected to reduce detection limits below those required for individual pesticide detection.

The IOSPR immunoprobe has the advantages of a short transducer length, small sample volume and the use of a gold film for surface attachment. The device also offers potential for further miniaturisation, for integration into arrays for single-chip multianalyte systems and for electrochemical applications.

Acknowledgements

The authors gratefully acknowledge the financial support of the EU Environment and Climate Programme, contract number EV5V-CT92-0067. The Optoelectronics Research Centre is an Interdisciplinary Research Centre supported by the UK Engineering and Physical Sciences Research Council.

References

Anemogiannis, E., Glytsis, E.N., 1992. Multilayer waveguides: efficient numerical analysis of general structures. J. Lightwave Technol. 10, 1344–1351.

Bester, K., Hühnerfuss, H., 1993. Triazines in the Baltic and North Sea. Marine Pollut. Bull. 26, 423–427.

Bier, F.F., Schmid, R.D., 1994. Real time analysis of competitive binding using grating coupler immunosensors for pesticide detection. Biosens. Bioelectron. 9, 125–130.

Brecht, A., Piehler, J., Lang, G., Gauglitz, G., 1995. A direct optical immunosensor for atrazine detection. Anal. Chim. Acta 311, 289–299.

Conte, S.D., De Boor, C., 1972. Elementary Numerical Analysis: an Algorithmic Approach, 2. McGraw-Hill, New York.

Delves, L., Lyeness, J., 1967. A numerical method for locating the zeros of an analytical function. Math. Comp. 21, 543–560.

Drapp, B., Piehler, J., Brecht, A., Gauglitz, G., Luff, B.J., Wilkinson, J.S., 1997. Mach-Zehnder interferometers as simazine immunoprobes. Sens. Actuators B 39, 277–282.

European Community, 1980. Council directive on the quality of water for human consumption. Official Journal of the EC, 80/778 EEC L229, 11.

Fattinger, Ch., Koller, H., Schlatter, D., Wehrli, P., 1993. The difference interferometer: a highly sensitive optical probe for quantification of molecular surface concentration. Biosens. Bioelectron. 8, 99–107.

Goddard, N.J., Pollard-Knight, D., Maule, C.H., 1994. Real-time biomolecular interaction analysis using the resonant mirror sensor. Analyst 119, 583–588.

Goss, C.A., Charych, D.H., Majda, M., 1991. Application of (3-mercaptopropyl)trimethoxysilane as a molecular adhesive in the fabrication of vapor-deposited gold electrodes on glass substrates. Anal. Chem. 63, 85–88.

Harris, R.D., Luff, B.J., Wilkinson, J.S., Wilson, R., Schiffrin, D.J., 1995a. Waveguide Surface Plasmon Resonance Biosensor for the Aqueous Environment. In: Proceedings of the Seventh European Conference on Integrated Optics (ECIO), Delft, The Netherlands, pp. 449–452.

Harris, R.D., Wilkinson, J.S., 1995b. Waveguide surface plasmon resonance sensors. Sens. Actuators B 29, 261–267.

Harris, R.D., Luff, B.J., Wilkinson, J.S., Wilson, R., Schiffrin, D.J., Piehler, J., Brecht, A., Abuknesha, R.A., Mouvet, C., 1996. Waveguide surface plasmon resonance biosensor for simazine analysis. In: Proceedings of the 11th International Conference on Optical Fiber Sensors (OFS 11), Sapporo, Japan, pp. 406–409.

Harris, R.D., 1996b. PhD Thesis, Southampton University, UK.

Heideman, R.G., Kooyman, R.P.H., Greve, J., 1993. Performance of a highly sensitive optical waveguide Mach-Zehnder interferometer immunosensor. Sens. Actuators B 10, 209–217.

Ingenhoff, J., Drapp, B., Gauglitz, G., 1993. Biosensors using integrated optical devices. Fresenius J. Anal. Chem. 346, 580–583.

Lavers, C.R., Harris, R.D., Hao, S., Wilkinson, J.S., O'Dwyer, K., Brust, M., Schiffrin, D.J., 1995. Electrochemically-controlled waveguide-coupled surface plasmon sensing. J. Electroanal. Chem. 387, 11–22.

Luff, B.J., Harris, R.D., Wilkinson, J.S., 1995. Directional coupler sensor using a low-index fluoropolymer isolation layer. In: Proceedings of the Seventh European Conference on Integrated Optics (ECIO), Delft, Holland, pp. 169–172.

Luff, B.J., Harris, R.D., Wilkinson, J.S., Wilson, R., Schiffrin, D.J., 1996a. Integrated optical directional coupler biosensor. Opt. Lett. 21, 618–620.

Luff, B.J., Harris, R.D., Wilkinson, J.S., Piehler, J., Brecht, A., Abuknesha, R.A., 1996b. Integrated optical directional coupler sensor for pesticide analysis. In: Proceedings of the International

Conference on Applications of Photonic Technology (ICAPT'96), Montreal, Canada.

Lukosz, W., 1991a. Principles and sensitivities of integrated optical and surface plasmon sensors for direct affinity sensing and immunosensing. Biosens. Bioelectron. 6, 215–225.

Lukosz, W., Clerc, D., Nellen, Ph.M., Stamm, Ch., Weiss, P., 1991b. Output grating couplers on planar optical waveguides as direct immunosensors. Biosens. Bioelectron. 6, 227–232.

Minunni, M., Mascini, M., 1993. Detection of pesticide in drinking water using real-time biospecific interaction analysis (BIA). Anal. Lett. 26, 1441–1460.

Mouvet, C., Broussard, S., Jeannot, R., Maciag, C., Abuknesha, R., Ismail, G., 1995. Validation of commercially available ELISA microtiter plates for triazines in water samples. Anal. Chim. Acta 311, 331–339.

Mouvet, C., Amalric, L., Broussard, S., Lang, G., Brecht, A., Gauglitz, G., 1996. Reflectometric interference spectroscopy for the determination of atrazine in natural water samples. Environ. Sci. Technol. 30, 1846–1851.

Mouvet, C., Harris, R.D., Maciag, C., Luff, B.J., Wilkinson, J.S., Piehler, J., Brecht, A., Gauglitz, G., Abuknesha, R.A., 1997. Determination of simazine in water samples by waveguide surface plasmon resonance. Anal. Chim. Acta 338, 109–117.

Piehler, J., Brecht, A., Geckeler, K.E., Gauglitz, G., 1996. Surface modification for direct immunoprobes. Biosens. Bioelectron. 11, 579–590.

Schlatter, D., Garner, R., Fattinger, Ch., Huber, W., Hubscher, J., Hurst, J., Koller, H., Mangold, C., Muller, F., 1993. The difference interferometer: application as a direct affinity sensor. Biosens. Bioelectron. 8, 109–116.

Stamm, Ch., Lukosz, W., 1993. Integrated optical difference interferometer as refractometer and chemical sensor. Sens. Actuators B 11, 177–181.

Syms, R.R.A., Cozens, J.R., 1992. Optical Guided Waves and Devices. McGraw-Hill, London.

Watterson, A., 1991. Pesticides and Your Food. Green Print, London.

Weast, R.C. (Ed.), 1971. Handbook of Chemistry and Physics, 52nd. ed. Chemical Rubber Company, Cleveland, OH.